

Supplement of Atmos. Chem. Phys., 19, 3125–3135, 2019
<https://doi.org/10.5194/acp-19-3125-2019-supplement>
© Author(s) 2019. This work is distributed under
the Creative Commons Attribution 4.0 License.



Atmospheric
Chemistry
and Physics
Open Access
EGU

Supplement of

A mechanism for biogenic production and emission of MEK from MVK decoupled from isoprene biosynthesis

Luca Cappellin et al.

Correspondence to: Luca Cappellin (luca.cappellin@gmail.com)

The copyright of individual parts of the supplement might differ from the CC BY 4.0 License.

S.1 Complementary GC-MS analysis of MVK transformation products

In order to support compound identification of MVK transformation products by red oak plants, the MVK fumigation experiments described in the main text were repeated with some minor modifications to include qualitative analysis by solid phase microextraction - gas chromatography – mass spectrometry (SPME-GC-MS). As depicted in Figure S1, MEK and 2-butanol were unambiguously identified as MVK transformation products by red oaks, confirming the results obtained using PTR/SRI-ToF-MS (Figure 1 of the main text). Similar results were obtained on *Hedera helix* and *Vitis vinifera* (Figure S1). No other putative MVK transformation products were detected by the SPME-GC-MS analysis. In particular, 3-buten-2-ol was below detection limit. At the contrary, the corresponding PTR-ToF-MS analysis reported in Figure 1 and Table S1, besides MEK and 2-butanol, also detected a small but statistically significant emission of 3-buten-2-ol (Table S1). The identification of the PTR-ToF-MS signal corresponding to the ion $C_4H_7^+$ as 3-buten-2-ol, besides being consistent with measurements using the pure compound standard (3-buten-2-ol undergoes protonation followed by dehydration upon reaction with H_3O^+), has also theoretical reasons. Ketones have been reported to be transformed by plants via reduction reactions (Kergomard et al., 1988). Hence MEK and 3-buten-2-ol are expected as MVK transformation products. Moreover, reduction reactions occur for MACR, producing in particular isobutyraldehyde and 2-methyl alcohol (Figure 1, Table S1, and Muramoto *et al.* (2015)).

15

S.1.1 Experimental setup for SPME-GC-MS analysis

The plant management and experimental setup was analogous to the one described in main text with the addition of a SPME fiber in the VOC-bag for collecting VOC for subsequent GC-MS analysis. No PTR/SRI-ToF-MS measurements were performed in this case. The experiment was repeated on six plants (four *Quercus rubra*, one *Hedera helix*, one *Vitis vinifera*). The GC-MS analysis was carried out as follows.

20

Headspace volatile compounds were collected by a 2 cm Solid Phase Microextraction fibre coated with divinylbenzene/carboxen/polydimethylsiloxane 50/30 μm (DBV/CAR/PDMS, Sigma-Adrich, St. Lewis, USA), inserted through the VOC-bag using a manual holder. The fibre was exposed to the headspace air through the duration of the fumigation. Volatile compounds adsorbed on the SPME fibre were desorbed at 250°C in the injector port of a GC interfaced with a mass detector (GC Agilent 7820A with Agilent 5977B MSD, Agilent Technologies, Santa Clara CA, USA). The mass detector was operated in electron ionization mode (EI, internal ionization source; 70 eV) with scan range from m/z 25–200. Separation was achieved on a Supelco SPB-624 capillary column (20 m x 0.18 mm ID x 1 μm film thickness; Sigma-Adrich, St. Lewis, USA). The GC oven temperature program consisted in 40°C for 6 min, then 40–200°C at 40°C min^{-1} , and stable at 200°C for 5 min. Helium was used as the carrier gas with a constant column flow rate of 0.8 mL min^{-1} . Compound identification was based on mass spectra matching with the standard NIST libraries (NIST 2.2 2014) and retention times of authentic reference standards.

30

References

- Cappellin, L., Biasioli, F., Granitto, P. M., Schuhfried, E., Soukoulis, C., Costa, F., Märk, T. D. and Gasperi, F.: On data analysis in PTR-TOF-MS: From raw spectra to data mining, *Sens. Actuators B Chem.*, 155(1), 183–190, doi:10.1016/j.snb.2010.11.044, 2011.
- 5 Cappellin, L., Karl, T., Probst, M., Ismailova, O., Winkler, P. M., Soukoulis, C., Aprea, E., Märk, T. D., Gasperi, F. and Biasioli, F.: On Quantitative Determination of Volatile Organic Compound Concentrations Using Proton Transfer Reaction Time-of-Flight Mass Spectrometry, *Env. Sci Technol.*, 46(4), 2283–2290, doi:10.1021/es203985t, 2012.
- Jordan, A., Haidacher, S., Hanel, G., Hartungen, E., Herbig, J., Märk, L., Schottkowsky, R., Seehauser, H., Sulzer, P. and Märk, T. D.: An online ultra-high sensitivity Proton-transfer-reaction mass-spectrometer combined with switchable reagent ion capability (PTR + SRI – MS), *Int. J. Mass Spectrom.*, 286(1), 32–38, doi:10.1016/j.ijms.2009.06.006, 2009.
- 10 Kergomard, A., Renard, M. F., Veschambre, H., Courtois, D. and Petiard, V.: Reduction of α,β -unsaturated ketones by plant suspension cultures, *Phytochemistry*, 27(2), 407–409, doi:10.1016/0031-9422(88)83108-X, 1988.
- Loreto, F. and Sharkey, T. D.: A gas-exchange study of photosynthesis and isoprene emission in *Quercus rubra*, *Planta*, 182(4), 523–531, doi:10.1007/BF02341027, 1990.
- 15 Muramoto, S., Matsubara, Y., Mwenda, C. M., Koeduka, T., Sakami, T., Tani, A. and Matsui, K.: Glutathionylation and Reduction of Methacrolein in Tomato Plants Account for Its Absorption from the Vapor Phase, *Plant Physiol.*, 169(3), 1744–1754, doi:10.1104/pp.15.01045, 2015.

Supplementary tables

Table S1. Total net flux in the fumigation experiments reported in Figure 1 (main text). Positive values denote net emission while negative values denote net uptake. Results are obtained by integrating the net flux curves reported in Figure 1. Results are reported as *mean ± se*.

<i>Fumigation with MVK</i>		
	TOTAL NET FLUX ($\mu\text{gC}/\text{m}^2$)	% of MVK uptake
MVK	-836 ± 257	
MEK	659 ± 242	73% ± 6%
3-buten-2-ol	38 ± 13	4% ± 0.4%
2-butanol	207 ± 32	19% ± 2%
MEK + 3-buten-2-ol + 2-butanol	839 ± 281	97% ± 4%
<i>Fumigation with MEK</i>		
	TOTAL NET FLUX ($\mu\text{gC}/\text{m}^2$)	% of MEK uptake
MVK	n.d.	
MEK	-270 ± 53	
3-buten-2-ol	n.d.	
2-butanol	171 ± 34	87% ± 13%
<i>Fumigation with 2-butanol</i>		
	TOTAL NET FLUX ($\mu\text{gC}/\text{m}^2$)	% of 2-butanol uptake
MVK	n.d.	
MEK	47 ± 6	90% ± 29%
3-buten-2-ol	n.d.	
2-butanol	-63 ± 10	
<i>Fumigation with 3-buten-2-ol</i>		
	TOTAL NET FLUX ($\mu\text{gC}/\text{m}^2$)	% of 3-buten-2-ol uptake
MVK	n.d.	
MEK	33 ± 7	33% ± 10%
3-buten-2-ol	-107 ± 10	
2-butanol	14 ± 2	14% ± 4%
MEK + 2-butanol	48 ± 9	47% ± 14%
<i>Fumigation with MACR</i>		
	TOTAL NET FLUX ($\mu\text{gC}/\text{m}^2$)	% of MACR uptake
MACR	-431 ± 110	
Isobutyraldehyde	33 ± 9	6.5% ± 0.8% (6.4%*)
2-Methallyl alcohol	4 ± 1	0.7% ± 0.3% (1.1%*)
Isobutanol	10 ± 1	2.1% ± 0.3% (1.8%*)
Isobutyraldehyde + 2-Methallyl alcohol + Isobutanol	48 ± 11	9.3% ± 0.8%

* Results in brackets represents values reported by Muramoto et al. (2015) in similar experiments using tomato plants.

Table S2. Spectral peaks and corresponding ions in PTR/SRI-TOF-MS for H₃O⁺ mode and NO⁺ mode. The mass resolving power of the PTR/SRI-ToF-MS (> 4000) and the peak deconvolution algorithm used (Cappellin et al., 2011) allowed to resolve the peaks reported in this table in each mode.

Compound	H3O+ mode		NO+ mode		
	m/z	Ion sum formula	m/z	Ion sum formula	
Isoprene	69.07	C ₅ H ₈ H ⁺	68.062	C ₅ H ₈ ⁺	
	70.0732	¹³ CC ₄ H ₈ H ⁺	69.0654	¹³ CC ₄ H ₈ ⁺	
	71.0766	¹³ C ₂ C ₃ H ₈ H ⁺	70.069	¹³ C ₂ C ₃ H ₈ ⁺	
	72.0844	¹³ C ₃ C ₂ H ₈ H ⁺	71.0721	¹³ C ₃ C ₂ H ₈ ⁺	
	73.0833	¹³ C ₄ CH ₈ H ⁺	72.0754	¹³ C ₄ CH ₈ ⁺	
	74.0866	¹³ C ₅ H ₈ H ⁺	73.0788	¹³ C ₅ H ₈ ⁺	
			98.06	C ₅ H ₈ ·NO ⁺	
			99.0634	¹³ CC ₄ H ₈ ·NO ⁺	
			100.0667	¹³ C ₂ C ₃ H ₈ ·NO ⁺	
			101.0701	¹³ C ₃ C ₂ H ₈ ·NO ⁺	
			102.0734	¹³ C ₄ CH ₈ ·NO ⁺	
			103.0768	¹³ C ₅ H ₈ ·NO ⁺	
	MVK	71.0491	C ₄ H ₆ OH ⁺	100.0393	C ₄ H ₆ O·NO ⁺
		72.0525	¹³ CC ₃ H ₆ OH ⁺	101.0427	¹³ CC ₃ H ₆ O·NO ⁺
73.0558		¹³ C ₂ C ₂ H ₆ OH ⁺	102.046	¹³ C ₂ C ₂ H ₆ O·NO ⁺	
74.0592		¹³ C ₃ CH ₆ OH ⁺	103.0494	¹³ C ₃ CH ₆ O·NO ⁺	
75.0626		¹³ C ₄ H ₆ OH ⁺	104.0527	¹³ C ₄ H ₆ O·NO ⁺	
MEK	73.0648	C ₄ H ₈ OH ⁺	102.05495	C ₄ H ₈ O·NO ⁺	
	74.0681	¹³ CC ₃ H ₈ OH ⁺	103.0583	¹³ CC ₃ H ₈ O·NO ⁺	
	75.0715	¹³ C ₂ C ₂ H ₈ OH ⁺	104.0627	¹³ C ₂ C ₂ H ₈ O·NO ⁺	
	76.0748	¹³ C ₃ CH ₈ OH ⁺	105.065	¹³ C ₃ CH ₈ O·NO ⁺	
	77.0782	¹³ C ₄ H ₈ OH ⁺	106.0684	¹³ C ₄ H ₈ O·NO ⁺	
3-buten-2-ol	55.0542	C ₄ H ₇ ⁺	71.0491	C ₄ H ₇ O ⁺	
	56.0576	¹³ CC ₃ H ₇ ⁺	72.0525	¹³ CC ₃ H ₇ O ⁺	
	57.0609	¹³ C ₂ C ₂ H ₇ ⁺	73.0558	¹³ C ₂ C ₂ H ₇ O ⁺	
	58.0643	¹³ C ₃ CH ₇ ⁺	74.0592	¹³ C ₃ CH ₇ O ⁺	
	59.0676	¹³ C ₄ H ₇ ⁺	75.0626	¹³ C ₄ H ₇ O ⁺	
2-butanol	57.07	C ₄ H ₉ ⁺	73.0648	C ₄ H ₉ O ⁺	
	58.0732	¹³ CC ₃ H ₉ ⁺	74.0681	¹³ CCH ₉ O ⁺	
	59.0766	¹³ C ₂ C ₂ H ₉ ⁺	75.0715	¹³ C ₂ C ₂ H ₉ O ⁺	
	60.0799	¹³ C ₃ CH ₉ ⁺	76.0748	¹³ C ₃ CH ₉ O ⁺	
	61.0833	¹³ C ₄ H ₉ ⁺	77.0782	¹³ C ₄ H ₉ O ⁺	

Figure captions

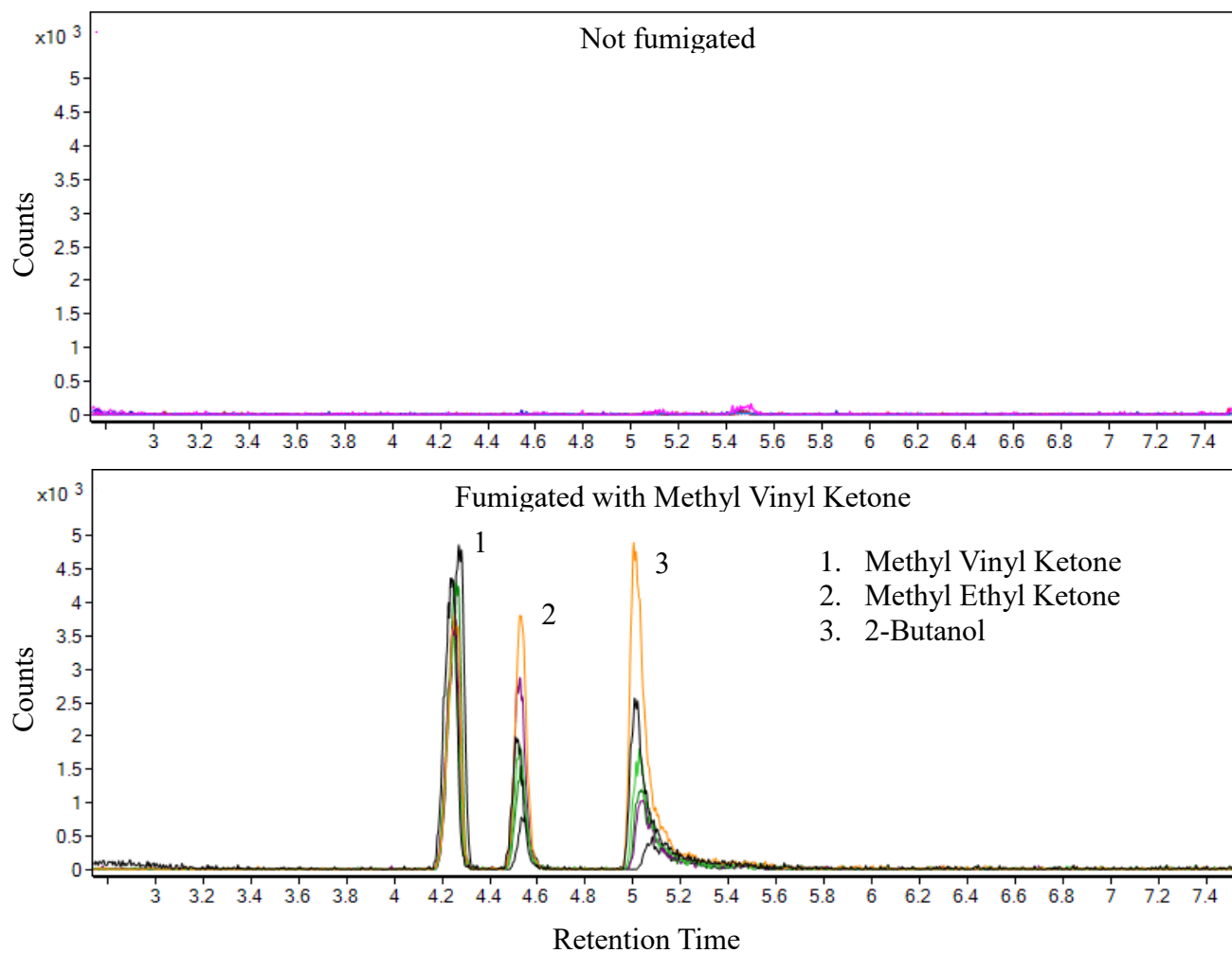


Figure S1. Excerpt of qualitative GC-MS analysis of six untreated plants (upper figure) and of the same plants fumigated with MVK (lower figure, $n=6$). The reported chromatograms correspond to $m/z = 45$ Th, so that all relevant peaks are clearly visible.

- 5 Different colours indicate different plants (yellow for *Hedera helix*; black for *Vitis vinifera*; other colours for *Quercus rubra*). Upon MVK fumigation, MEK and 2-butanol were formed by all plants, while 3-buten-2-ol was below detection limit and could only be detected by PTR-ToF-MS (Table S1). No other MVK transformation compounds were detected by GC-MS. Such data is reported to support compound identification for the fumigation experiments reported in the main text (Figure 1).

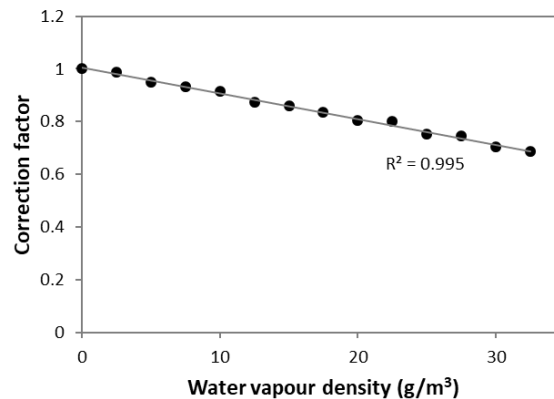
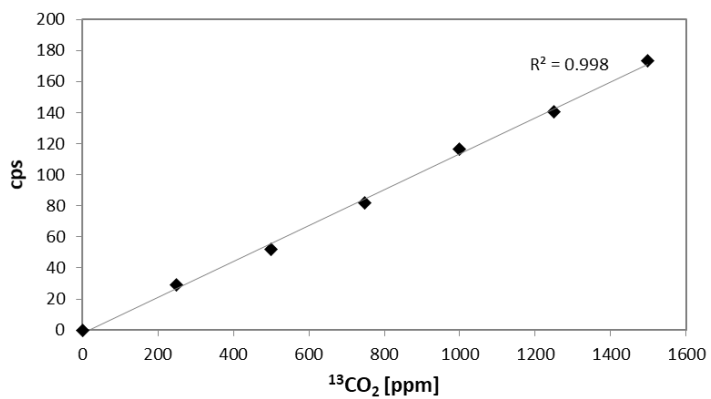


Figure S2. Left: Example of calibration curve for $^{13}\text{CO}_2$ detected as protonated $^{13}\text{CO}_2$ ($m/z = 46.005$ Th) at dry conditions. Right: Experimentally determined correction factors for the $^{13}\text{CO}_2$ sensitivity as a function of the water vapour density.

5